

Tuning the magnetic properties of half-metallic semi-Heusler alloys by *sp*-electron substitution: The case of $\text{AuMnSn}_{1-x}\text{Sb}_x$ quaternary alloys

K. Özdoğan^{1,*}, I. Galanakis^{2,†} and E. Şaşıoğlu^{3,4‡}

¹ *Department of Physics, Gebze Institute of Technology, Gebze, 41400, Kocaeli, Turkey*

² *Department of Materials Science, School of Natural Sciences, University of Patras, GR-26504 Patras, Greece*

³ *Institut für Festkörperforschung, Forschungszentrum Jülich, D-52425 Jülich, Germany*

⁴ *Fatih University, Physics Department, 34500, Büyükcçekmece, İstanbul, Turkey*

(Dated: December 17, 2020)

We study the electronic and magnetic properties of the quaternary $\text{AuMnSn}_{1-x}\text{Sb}_x$ Heusler alloys using first principles calculations. We determine their magnetic phase diagram and we show that they present a phase transition from a ferromagnetic to an antiferromagnetic state with increasing Sb concentration. For large Sb concentrations the antiferromagnetic superexchange coupling dominates over the ferromagnetic RKKY-like exchange mechanism. This behavior is similar to the one demonstrated by the isovalent $\text{Ni}_{1-x}\text{Cu}_x\text{MnSb}$ alloy studied recently by the authors [I. Galanakis et al, Phys. Rev. B. **77**, 214417 (2008)]. Thus the variation of the concentration of the *sp*-electrons (Sn and Sb atoms) and the variation of the concentration of the non-magnetic *3d* atoms (Cu) lead to a similar tuning of the the magnetic properties of the Heusler alloys. We show that the inclusion of correlation effects does not alter the phase diagram. Calculated results are in good agreement with the available experimental data.

PACS numbers: 75.50.Cc, 75.30.Et, 71.15.Mb

Semi-Heusler alloys with the chemical formula XYZ are ternary compounds consisting of two different transition metals (X and Y) and one *sp* element (Z), and crystallize in the $C1_b$ structure. Their name stems from von Heusler who first studied the Cu-Mn-Al system in 1903.¹ The interest on these alloys has been recently revived due the half-metallic character exhibited by some semi-Heuslers; i.e. compounds for which one spin channel is semiconducting or insulating whereas the other has a metallic character, leading to 100% carrier spin-polarization at the Fermi level (E_F). Half-metallic ferromagnetism (HMF) was initially proposed by de Groot et al. in 1983 when studying the band structure of the NiMnSb Heusler compound.² Also members of the family of the so-called full-Heusler alloys like Co_2MnZ (Z=Si and Ge) have been predicted to be half-metals.³

Early measurements by Webster et al. on several quaternary Heusler alloys, as well as recent studies of Walle et al. on $\text{AuMnSn}_{1-x}\text{Sb}_x$, demonstrated the importance of the *sp* electrons in establishing the magnetic properties of Heusler compounds.^{4,5} On the other hand, the importance of the non-magnetic *3d* atoms, like Cu, for the magnetism of Heusler alloys has been also revealed recently by the experimental studies of Duong et al. and Ren et al. in the case of $\text{Co}_{1-x}\text{Cu}_x\text{MnSb}$ and $\text{Ni}_{1-x}\text{Cu}_x\text{MnSb}$ alloys, respectively.^{6,7}

Authors have shown in Ref. 8 that when Ni atoms are substituted by Cu ones in the half-metallic NiMnSb alloy, first the half-metallicity is lost and for large Cu concentrations the $\text{Ni}_{1-x}\text{Cu}_x\text{MnSb}$ alloys become antiferromagnetic; the phase transition occurs for a concentration $x \simeq 0.6$. We have to note here that CuMnSb is a well-known antiferromagnet and has been extensively studied both experimentally⁹ and theoretically.¹⁰ The exchange coupling mechanism in Mn-based Heusler alloys

has been well-understood¹¹ and for half-metallic systems it has been shown in Ref. 8 that the magnetic interactions depend strongly on the position of the Fermi level within the gap. As the concentration in Cu is increasing the Fermi level is shifted higher in energy with respect to the minority-spin gap and at the transition point it crosses enough the minority-spin conduction band so that the antiferromagnetic superexchange coupling of the Mn-Mn spin moments through the Cu atoms dominates over the ferromagnetic RKKY-like interaction between the Mn atoms.

In the semi-Heusler alloys of the chemical type AuMnZ (Z=In, Sn, Sb), the magnetization is confined to the Mn sublattice and the Mn spin moments are well-localized in space due to the large Mn-Mn distance, i.e. the *3d* states belonging to different Mn atoms do not overlap considerably. M. Amft and P. M. Oppeneer calculated the largest zero-temperature polar Kerr rotation (-0.45 degree at about 1 eV photon energy) for AuMnSn .¹² AuMnSn alloy is isovalent (same number of valence electrons in the primitive unit cell) to NiMnSb and AuMnSb is isovalent to CuMnSb . Thus the phase magnetic diagram of $\text{AuMnSn}_{1-x}\text{Sb}_x$ and $\text{Ni}_{1-x}\text{Cu}_x\text{MnSb}$ compounds can be directly compared. In this Brief Report we employ the full-potential nonorthogonal local-orbital minimum-basis band structure scheme (FPLO)¹³ within the local density approximation (LDA)¹⁴ to study the phase diagram of the quaternary $\text{AuMnSn}_{1-x}\text{Sb}_x$ alloys and compare it with our published results on $\text{Ni}_{1-x}\text{Cu}_x\text{MnSb}$ compounds. We simulate the disorder within the the coherent potential approximation (CPA) framework. Details of the calculations are similar to the ones presented in Ref. 8. We have used the theoretical calculated equilibrium lattice constants: 5.83 Å for NiMnSb , 5.99 Å for CuMnSb , 6.333 Å for AuMnSn , and 6.464 Å for AuMnSb .

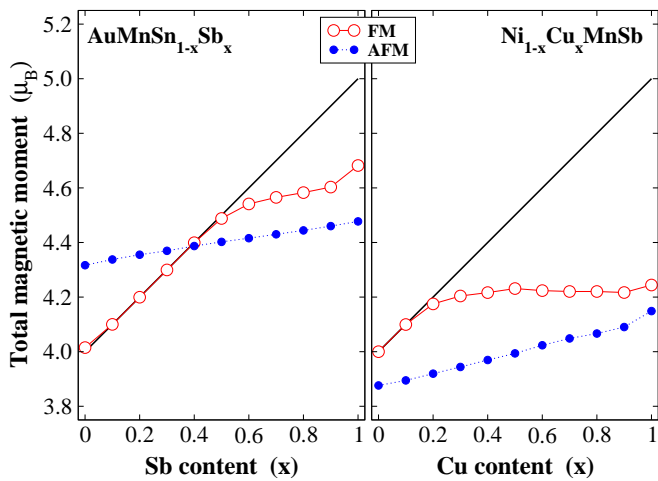


FIG. 1: (Color online) Calculated total spin moments (in μ_B) as a function of the concentration (x) for the studied $\text{AuMnSn}_{1-x}\text{Sb}_x$ and $\text{Ni}_{1-x}\text{Cu}_x\text{MnSb}$ in the ferromagnetic (FM) configuration. We present also the Mn spin moment in the antiferromagnetic (AFM) configurations for comparison. The solid black lines represent the Slater-Pauling behavior.

These are slightly different than the experimental ones: 5.93 Å for NiMnSb, 6.09 Å for CuMnSb, 6.341 Å for AuMnSn and 6.379 Å for AuMnSb.^{4,15} We should note here that we performed test calculations also for the experimental lattice constants but results were almost identical to the case of the theoretical lattice parameters. We assumed that the lattice constant for the quaternary alloys varies linearly with the concentration x . We show that $\text{AuMnSn}_{1-x}\text{Sb}_x$ alloys present a similar magnetic phase diagram with the $\text{Ni}_{1-x}\text{Cu}_x\text{MnSb}$ compounds and the tuning of the magnetic properties is insensitive to the origin of the conduction electrons which mediate the Mn-Mn interactions.

We will start our discussion from the calculated spin magnetic moments presented in Fig. 1. We have drawn the total magnetic moments for the $\text{AuMnSn}_{1-x}\text{Sb}_x$ and $\text{Ni}_{1-x}\text{Cu}_x\text{MnSb}$ alloys as a function of the concentration for the ferromagnetic state in Fig. 1. The solid black lines represent the Slater-Pauling (SP) behavior obeyed by the perfect half metallic ferromagnets (the total spin moment in μ_B is the number of valence electrons minus 18)¹⁶. We present the Mn magnetic moment corresponding to the antiferromagnetic state for comparison. We should note that the spin magnetic moments of Au, Ni and Cu are zero in the antiferromagnetic (AFM) state due to symmetry reasons while the Sb and Sn atoms have a very small magnetic moment value. For $x = 0$ the AuMnSn compound has a total spin moment slightly larger than the ideal $4 \mu_B$ predicted by the SP rule for the perfect half-metallic ferromagnets since the Fermi level is slightly below the gap as can be seen in Fig. 2 where we have drawn the total density of state (DOS) for both families of compounds. NiMnSb is an ideal half-metal and this is reflected on an integer value of the total spin

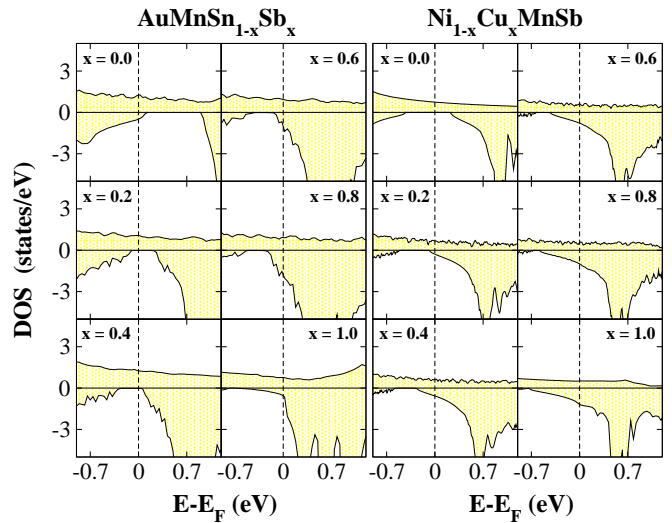


FIG. 2: (Color online) Spin-resolved total density of states (DOS) in the case of the $\text{AuMnSn}_{1-x}\text{Sb}_x$ (left panel) and $\text{Ni}_{1-x}\text{Cu}_x\text{MnSb}$ (right panel) around the Fermi level for selected values of x . We have set the Fermi level as the zero of the energy axis. Positive values of DOS correspond to the majority-spin electrons and negative values to the minority-spin electrons.

magnetic moment which is $4 \mu_B$ and the Fermi level is located in the middle of the gap. The $\text{AuMnSn}_{1-x}\text{Sb}_x$ and $\text{Ni}_{1-x}\text{Cu}_x\text{MnSb}$ follow the SP rule up to $x \simeq 0.5$ and $x \simeq 0.2$, respectively, and at this point the half-metallicity is lost since the Fermi level is shifted and now crosses the minority-spin conduction band. This is clearly shown in Fig. 2. The shift of the Fermi level towards higher energies is easily understood. When we increase the concentration of Sb and Cu atoms, we dope the system with p charge. The corresponding majority-spin p states are extremely extended in energy and thus, when their occupation increases, they push the Fermi level higher in energy.

To reveal the mechanism for the loss of the half-metallic character we have to study the atom-resolved spin magnetic moments for the ferromagnetic configuration presented in Table I. The spin magnetic moment of Au, Sn and Sb atoms changes from -0.022, -0.155 and -0.100 to 0.118, -0.020 and 0.044 μ_B , respectively, with increasing of the Sb concentration in the $\text{AuMnSn}_{1-x}\text{Sb}_x$ compound. These atoms have almost filled electronic shells, since they provide electronic bands, much deeper in energy than the Mn ones,¹⁶ and they contribute marginally to the total spin moment. Thus the extra electron provided by the Sb atom has to be accommodated by the bands provided by the Mn atom. For AuMnSn, the spin magnetic moment of Mn is 4.192 μ_B and thus most of the five majority-spin states are occupied. To occupy further the Mn majority states costs a lot in energy and the system prefers to occupy partially also the minority-spin states above the gap and the half-metallicity is lost. As a result the Mn spin mo-

TABLE I: Total and atom-resolved spin magnetic moments in μ_B for the ferromagnetic configuration as a function of the concentration, x , in $\text{AuMnSn}_{1-x}\text{Sb}_x$ and $\text{Ni}_{1-x}\text{Cu}_x\text{MnSb}$ compounds. Values have been scaled to one atom.

x	$\text{AuMnSn}_{1-x}\text{Sb}_x$ (FM)					$\text{Ni}_{1-x}\text{Cu}_x\text{MnSb}$ (FM)				
	Total	Au	Mn	Sn	Sb	Total	Ni	Cu	Mn	Sb
0.0	4.015	-0.022	4.192	-0.155		4.000	0.255		3.847	-0.102
0.2	4.199	0.023	4.286	-0.117	-0.078	4.175	0.310	0.072	3.982	-0.070
0.4	4.399	0.064	4.392	-0.073	-0.033	4.216	0.324	0.078	4.042	-0.052
0.6	4.541	0.094	4.459	-0.038	0.004	4.224	0.327	0.080	4.083	-0.038
0.8	4.582	0.103	4.470	-0.026	0.018	4.220	0.327	0.083	4.113	-0.025
1.0	4.682	0.118	4.520		0.044	4.244		0.096	4.158	-0.010

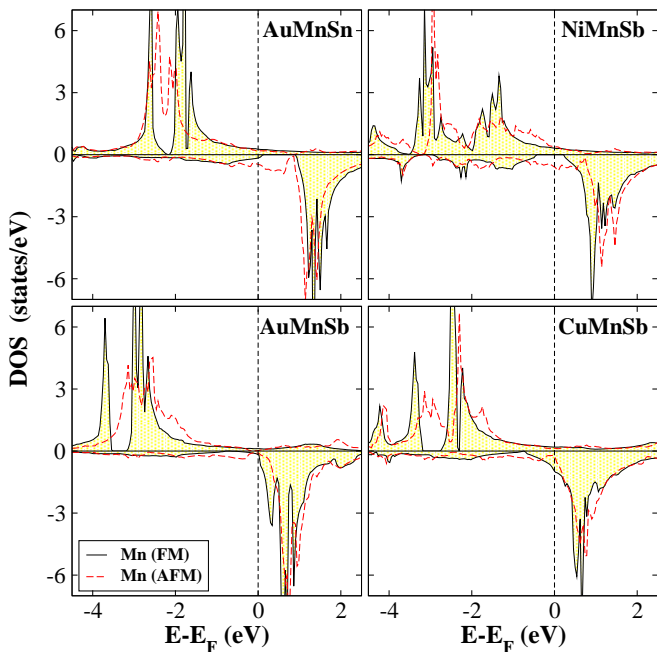


FIG. 3: (Color online) Spin-resolved Mn density of states (DOS) of CuMnSb , NiMnSb , AuMnSn and AuMnSb compounds for FM and AFM configurations.

ment is only around $0.32\mu_B$ larger in AuMnSb reaching a value of $4.520\mu_B$. The calculated magnetic moments are in good agreement with experimental values of AuMnSn^{17} and AuMnSb^{18} compounds. In the case of $\text{Ni}_{1-x}\text{Cu}_x\text{MnSb}$ alloys the same phenomenon occurs: Ni, Cu and Sb atoms carry very small spin moments and Mn increases its spin moment by $0.31\mu_B$ when all Ni atoms are substituted by Cu ones leading to the loss of the half-metallicity.

In the antiferromagnetic (AFM) state, Sb and Sn have a very small magnetic moment while the magnetic moment of Au is zero in $\text{AuMnSn}_{1-x}\text{Sb}_x$ compound due to symmetry reasons. Similarly in the case of the $\text{Ni}_{1-x}\text{Cu}_x\text{MnSb}$ alloys, Ni and Cu have zero spin moments, while Sb has a very small magnetic moment. The closeness in value between the Mn spin moments in FM and AFM configurations shown in Fig. 1 can be understood if we examine the Mn-resolved DOS shown for

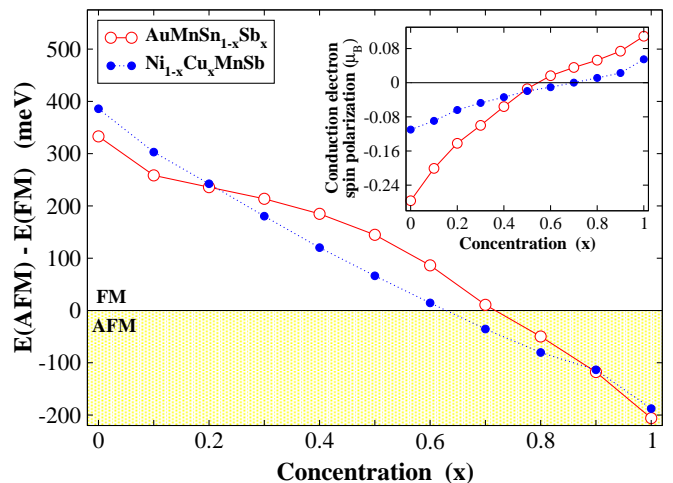


FIG. 4: (Color online) Ground state magnetic phase diagram and total energy differences between AFM and FM configurations of the Mn magnetic moments in $\text{AuMnSn}_{1-x}\text{Sb}_x$ and $\text{Ni}_{1-x}\text{Cu}_x\text{MnSb}$ as a function of the concentration (x). In the inset we show the total spin polarization of the conduction electrons of X (Au, Ni, Cu) and Z (Sn and Sb) atoms as a function of the concentration (x). Note that the energy differences are given for an antiferromagnetic unit cell, while spin polarization of the conduction electrons is given for a FM unit cell

all four CuMnSb , NiMnSb , AuMnSn and AuMnSb compounds in Fig. 3. Both in the FM and AFM cases Mn atoms present a similar DOS and the small broadening of the bands in the AFM state occurs due to the stronger hybridization with the other atoms in this case. The important point is that the similar DOS in the FM and AFM cases justifies the use of the Anderson $s-d$ model to interpret the results on the quaternary $\text{AuMnSn}_{1-x}\text{Sb}_x$ alloys as in Ref. 8 for the $\text{Ni}_{1-x}\text{Cu}_x\text{MnSb}$ alloys.

As we have mentioned above both $\text{AuMnSn}_{1-x}\text{Sb}_x$ and $\text{Ni}_{1-x}\text{Cu}_x\text{MnSb}$ quaternary compounds lose their half-metallic character at a concentration of $x \simeq 0.5$ and $x \simeq 0.2$, respectively. For these values of the concentration the Fermi level enters the minority-spin conduction band but the ferromagnetism is still favorable with respect to the AFM state. To study the phase transition, we have calculated the total energies for both the FM and the AFM configurations of the Mn spin mag-

netic moments. All energy calculations have been performed using the large AFM unit cell (which is double the FM unit cell). We determine the zero temperature magnetic phase diagram as the difference of the corresponding total energies ($E_{AFM} - E_{FM}$) per AFM unit cell and we present our results in Fig. 4. $\text{AuMnSn}_{1-x}\text{Sb}_x$ shows a phase transition from a FM to an AFM coupling of the Mn spin moments for a critical concentration value $x \simeq 0.7$. As seen in Figs. 2 and 3 when we substitute Sb for Sn, the Fermi level moves towards higher energies and the number of the minority states just above the Fermi level increases. This gives rise to an opposite behavior in the relative contributions of the exchange mechanisms: a decrease for the RKKY-like coupling and an increase in the superexchange mechanism. At the transition point both mechanisms cancel each other and further increase of x leads to an antiferromagnetic order due to the dominating character of the superexchange mechanism. The value for the transition for the $\text{AuMnSn}_{1-x}\text{Sb}_x$ alloys is very close to the transition value of $x \simeq 0.6$ calculated already for $\text{Ni}_{1-x}\text{Cu}_x\text{MnSb}$ in Ref. 8 and reproduced here. The similar behavior of the two families of alloys can be traced in the spin-polarization of the conduction electrons of the Au, Sn and Sb atoms (Ni, Cu, Sb in the case of $\text{Ni}_{1-x}\text{Cu}_x\text{MnSb}$) presented in the inset of Fig. 4 which is similar for both families of alloys. These electrons are responsible for the coupling between the distinct Mn localized spin magnetic moments. The role of the spin-polarization of the conduction electrons and their connection to the phase diagram have been largely discussed in Ref. 8.

We should finally note that we have examined also the influence of the electron-correlation on the magnetic phase diagram for the $\text{AuMnSn}_{1-x}\text{Sb}_x$ alloys taken into account using the popular LDA+ U scheme.¹⁹ We have assumed a value for the Mn exchange-splitting constant

J of 0.8 eV and have varied the on-site Coulomb repulsion constant U between 3 and 5 eV and calculated the $E_{AFM} - E_{FM}$ for AuMnSb . LDA+ U should push the Mn unoccupied minority states higher in energy similarly to the effect of the expansion of the lattice constant. But for AuMnSb this shift of the states is very small revealing that correlations do not play a crucial role for the description of these alloys. As a result the $E_{AFM} - E_{FM}$ varies between -156.15 and -155.39 meV as U changes from 3 to 5 eV (close to the value of ~ -200 meV when U is not included in the calculations) and the AFM state remains the ground state. Thus the inclusion of the correlations in our electronic-structure calculations only slightly shifts the transition point to lower Sb concentration.

We have studied the effect of the variation of the concentration of the sp electrons on the electronic and magnetic properties of the quaternary $\text{AuMnSn}_{1-x}\text{Sb}_x$ ($0 \leq x \leq 1$) Heusler alloys using first principles calculations. We determine their magnetic phase diagram and we show that they present a phase transition from a ferromagnetic to an antiferromagnetic state with increasing Sb concentration. For large Sb concentrations the antiferromagnetic superexchange coupling dominates over the ferromagnetic RKKY-like exchange mechanism. Electronic correlation effects have a marginal effect on the magnetic phase diagram of these compounds. This is an alternative route for tuning the magnetic properties of the Heusler alloys with respect to the variation of the non-magnetic $3d$ atoms shown for $\text{Ni}_{1-x}\text{Cu}_x\text{MnSb}$ alloys [I. Galanakis et al, Phys. Rev. B. **77**, 214417 (2008)]. These findings can be used as a practical tool to design materials with given physical properties.

Authors acknowledge the computer support of the Leibniz Institute for Solid State and Materials Research Dresden, and the assistance of Ulrike Nitzsche in using the computer facilities.

* Electronic address: kozdogan@gyte.edu.tr

† Electronic address: galanakis@upatras.gr

‡ Electronic address: e.sasioglu@fz-juelich.de

¹ F. Heusler, Verh. Dtsch. Phys. Ges **5**, 219 (1903).

² R. A. de Groot, F. M. Mueller, P. G. van Engen, and K. H. J. Buschow Phys. Rev. Lett. **50**, 2024 (1983).

³ S. Ishida, S. Fujii, S. Kashiwagi, and S. Asano J. Phys. Soc. Jpn. **64**, 2152 (1995); S. Fujii, S. Ishida, and S. Asano, J. Phys. Soc. Jpn. **64**, 185 (1995)

⁴ P. J. Webster and K. R. A. Ziebeck, in *Alloys and Compounds of d-Elements with Main Group Elements. Part 2.*, edited by H. R. J. Wijn, Landolt-Boörnstein, New Series, Group III, Vol. 19/c (Springer-Verlag, Berlin 1988).

⁵ C. Walle, L. Offernes, and A. Kjekshus, J. Alloys and Comp. **349**, 105 (2003).

⁶ N. P. Duong, L. T. Hung, T. D. Hien, N. P. Thuy, N. T. Trung, and E. Brück, J. Magn. Magn. Mater. **311**, 605 (2007).

⁷ S. K. Ren, W. Q. Zou, J. Gao, X. L. Jiang, F. M. Zhang, and Y. W. Du, J. Mag. Magn. Mater. **288**, 276 (2005).

⁸ I. Galanakis, Şaşıoğlu, and K. Özdoğan, Phys. Rev. B **77**, 214417 (2008).

⁹ J. Boëuf, C. Pfleiderer, and A. Faißt, Phys. Rev. B **74**, 024428 (2006).

¹⁰ T. Jeong, R. Weht, and W. E. Pickett, Phys. Rev. B **71**, 184103 (2005).

¹¹ E. Şaşıoğlu, L. M. Sandratskii, and P. Bruno, Appl. Phys. Lett. **89**, 222508 (2006); *ibid.* Phys. Rev. B **77**, 064417 (2008).

¹² M. Amft and P. M. Oppeneer J. Phys. Condens. Mat. **19**, 315216 (2007).

¹³ K. Koepernik and H. Eschrig, Phys. Rev. B **59**, 3174 (1999); K. Koepernik, B. Velicky, R. Hayn, and H. Eschrig, Phys. Rev. B **58**, 6944 (1998).

¹⁴ J. P. Perdew and Y. Wang, Phys. Rev. B **45**, 13244 (1992).

¹⁵ L. Offernes, P. Ravindran and A. Kjekshus Appl. Phys. Lett. **82**, 17 (2003).

¹⁶ I. Galanakis, P. H. Dederichs, and N. Papanikolaou, Phys. Rev. B **66**, 134428 (2002).

¹⁷ A. Neumann, L. Offernes, and A. Kjekshus, J. Alloys and

- Comp. **274**, 136 (1998).
- ¹⁸ J. Pierre, R.V. Skolozdra, J. Tobola, S. Kaprzyk, C. Hord-equin, M. A. Kouacou, I. Karla, R. Currat and E. Lelivre-Berna, *J. Alloys and Comp.***101**, 262 (1997).
- ¹⁹ V. I. Anisimov, J. Zaanen, and O. K. Andersen, *Phys. Rev. B* **44**, 943 (1991).